

H. Slimani, A. Zeghoudi, A. Bendaoud, S. Bechekir

Experimental evaluation of conducted disturbances induced during high frequency switching of active components

Introduction. Power electronics devices are among the most widely used equipment in all fields. The increasing performance of these devices makes their electromagnetic interference factor very important. On the other hand, electromagnetic compatibility research is more and more interested in studies on the sources of electromagnetic disturbances, their propagation paths and the methods of reducing these electromagnetic disturbances. The **purpose** is to study the behavior of the various active power components at high frequency as well as the evaluation of their electromagnetic noise by using simulation and experimental measurement. **Methods.** In first time, the simulation was realized with the Lt-spice software which presents many advantages in its use and we validate in the second time the results obtained with experimental measurements. We start by study of the behavior of the diode, then the behavior of MOSFET transistor and finally the study of the behavior of the IGBT transistor. **Results.** All the simulations were performed using the Lt-spice software and the results obtained are validated by experimental measurements performed in the APELEC Laboratory at the University of Sidi Bel-Abbes in Algeria. The waveforms of the current and voltage across each component during its opening are presented. The results of the simulations are compared and validated with the realized measurements in order to better present the influence of the fast switching of semiconductors on the electrical quantities, which causes electromagnetic disturbances in the interconnected electrical system. References 19, figures 19.

Key words: electromagnetic compatibility, electromagnetic disturbances, high frequency switching of active components, experimental measurement.

Вступ. Пристрої силовій електроніки знаходяться серед обладнання, що найбільш широко використовується у всіх областях. Підвищення продуктивності цих пристроїв робить фактор їх електромагнітних перешкод дуже важливим. З іншого боку, при дослідженні електромагнітної сумісності дедалі більше цікавляться джерелами електромагнітних перешкод, шляхів їх поширення та методами зменшення цих електромагнітних перешкод. **Мета** роботи полягає в тому, щоб вивчити поведінку різних компонентів активної потужності на високих частотах, а також оцінити їхній електромагнітний шум за допомогою моделювання та експериментальних вимірювань. **Методи.** Уперше моделювання було реалізовано за допомогою програмного забезпечення Lt-spice, яке дає базато переваг при його використанні, і вдруге ми підтверджуємо результати, отримані за допомогою експериментальних вимірів. Ми починаємо з вивчення поведінки діода, потім поведінки MOSFET транзистора і, нарешті, вивчення поведінки IGBT транзистора. **Результати.** Усі моделювання були виконані з використанням програмного забезпечення Lt-spice, а отримані результати підтверджені експериментальними вимірами, проведеними в лабораторії APELEC в Університеті Сіді-Бель-Аббес в Алжирі. Представлені осцилограми струму та напруги на кожному компоненті під час його відкриття. Результати моделювання порівнюються та підтверджуються реалізованими вимірами, щоб краще уявити вплив швидкого перемикавання напівпровідників на електричні величини, що викликає електромагнітні перешкоди у взаємозалежній електричній системі. Бібл. 19, рис. 19.

Ключові слова: електромагнітна сумісність, електромагнітні перешкоди, високочастотне перемикавання активних елементів, експериментальне вимірювання.

Introduction. With the development of new sources of renewable energy, more static converters are connected to the power network. They supply of the network with electric power produced by generators; but in contrast to conventional systems, they usually introduce low frequency and high frequency (HF) switching harmonics [1-5]. These power converters use fast switching power semiconductor switches, such as MOSFET and IGBT transistors as the preferred switching devices because of their various properties, such as higher efficiency, smaller size, and lower overall cost, low losses associated with switching device. However, the fast switching speed of new converter technologies has the potential to cause electromagnetic disturbances and high dV/dt [6-9].

The orders of magnitude of the commutation gradients can vary between 100 to 1000 A/ μ s for the dI/dt and from 5 to 50 kV/ μ s for the dV/dt . Moreover, very high commutation frequency is another factor that increases the electromagnetic pollution, as it can vary from 100 Hz to 1 MHz. This condition presents a serious problem in regards to the Electromagnetic Compatibility (EMC) [10, 11].

The brutal variations of the voltage associated with parasitic elements between the system and the ground plane induce disturbing currents in the ground circuits.

To show the role that a switch can play in the plan [voltage $V(t)$ across the switch – current $i(t)$ through the switch] Fig. 1 shows:

- the feature branches where the switch can operate;
- the branch changes it can provide [10-12].

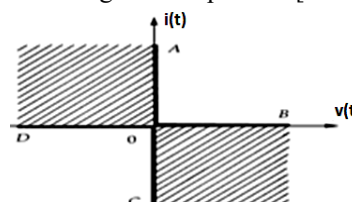


Fig. 1. Quadrants of the plan [$V(t)$, $i(t)$] [13]

The first step of evaluating the conducted emission interferences consist of determining the sources of these interferences. For this reason in this work we have made an evaluation of the conducted disturbances emitted during the HF switching of active components such as the diode, MOSFET, IGBT the study is made by simulation using the Lt-spice software and the experimental measurements by measurement benches carried out at the APELEC Laboratory at the University of Sidi Bel-Abbes.

The **purpose** of this article is to study the behavior of the various active power components at high frequency as well as the evaluation of their electromagnetic noise by using simulation and experimental measurement.

Study of the real behavior of active components. In this part of the work, the dynamic characteristics and the equivalent models of the real behavior for each component

© H. Slimani, A. Zeghoudi, A. Bendaoud, S. Bechekir

studied were presented. These components are: the diode, the MOSFET and IGBT transistors. Our objective is to know the influence of these elements on some electrical quantities at well determined switching times and the disturbances generated in the interconnected electrical system [13-15]. To do this, we will first study the switching cells (Fig. 2), which allows us to describe the operation of power electronics structures and also gives us a more detailed analysis of switching phenomena [16, 17]. The benches used have been developed for many years for the characterization of power components in switching whose operation has been largely validated by experimental measurements. In order to represent the switching characteristics of the components mentioned above, we have carried out simulations under Lt-spice software, where the results are validated by experimental measurements.

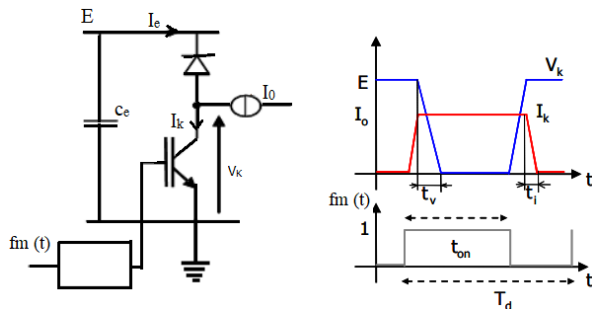


Fig. 2. Switching cell and associated waveforms

The main switch is controlled by a periodic modulation function $f_m(t)$ with T_d as the binary period value and $\alpha = t_{on}/T_d$ as a variable duty cycle. This duty cycle modulates the power transfer. For simplification, the external switching cell values (E, I_0) are considered constant while internal ones (I_e, V_k) are taken as variables modulated by the $f_m(t)$ function [3, 4]

Study of the behavior of the diode. For the identification of the dynamic characteristics of the diodes, we used the circuit presented in Fig. 3.

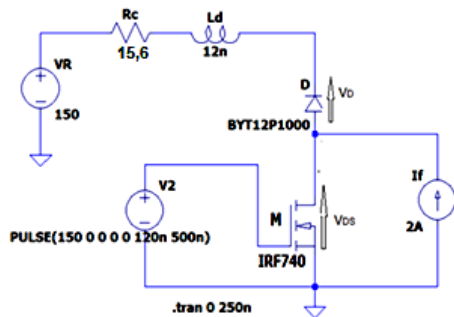


Fig. 3. Simulation diagram for the switching of a power diode, (M: IRF740, D: BYT12P1000)

This circuit presents the switching of a MOSFET/diode cell, in which the switch is a MOSFET transistor of type IRF740 connected with a diode of type BYT12P1000. For this simulation, we used directly the component models provided by the Lt-spice library. The inductance L_d represents the global parasitic inductances in the circuit [18, 19]. It is a series inductance introduced in particular by the legs of the diode in order to simulate the dynamic behavior of the diode. Figure 4 represents a photo of the measurement bench to compare the simulation results of the voltage across the diode and the current through it with the measurements.

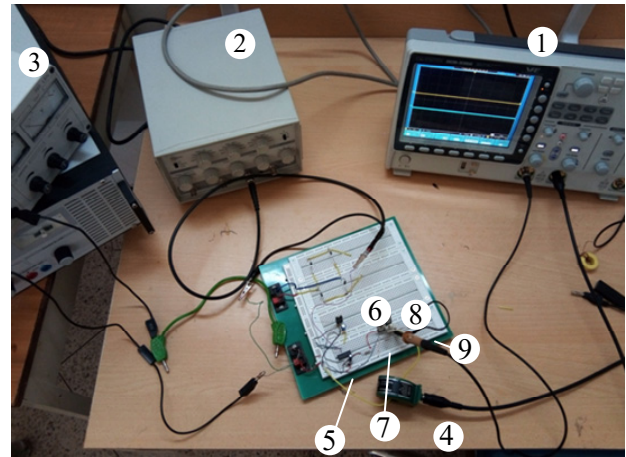


Fig. 4. Photo of the measurement bench [14]:
1 – oscilloscope; 2 – pulse generator; 3 – stabilized power supply; 4 – amperometric probe; 5 – driver IR2110; 6 – 12 V regulator; 7 – MOSFET IRF740; 8 – diode BYT12P1000; 9 – resistance 15,6 Ω

Figure 5 shows the descriptive diagram of the main elements used to switch a BYT12P1000 type power diode.

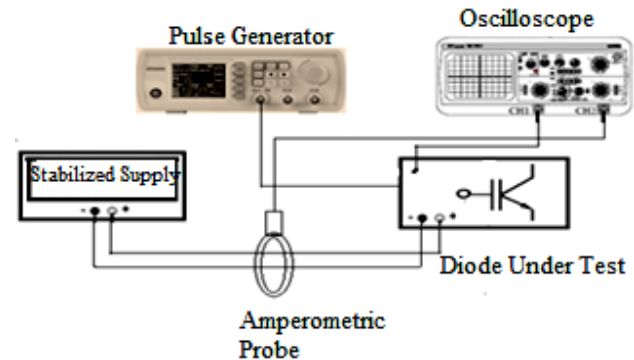


Fig. 5. Descriptive diagram of the test bench for switching a power diode

According to the diagram (Fig. 3), we can establish the equation that describes the mesh of this circuit [15]:

$$V_R = L_d \frac{di(t)}{dt} - V_D + V_{DS}, \quad (1)$$

where V_R is the source voltage; V_D is the voltage at the diode terminal; V_{DS} is the voltage between drain source of MOSFET; L_d represents the global parasitic inductances in the circuit.

If the MOSFET does not intervene during switching ($V_{DS} \ll V_R$), then we have:

$$V_R = L_d \frac{di(t)}{dt} - V_D. \quad (2)$$

The simulation diagram has the following characteristics: the current I_f generates by the current source $I_f = 2$ A, $V_R = 150$ V, $R_c = 15.6$ Ω ; $L_D = 12$ nH.

Results and analysis. Figures 6, 8 show the temporal variations in the blocking of the diode tested according to the simulation and measurements, they also illustrate the phenomenon of reverse overlap on the current and voltage when the diode is blocked. For the frequency response, the results are shown in Fig. 7, 9, where we note respectively a decrease of amplitude from 20 dB to -80 dB for the current and a decrease of amplitude from 30 dB to -70 dB for the voltage.

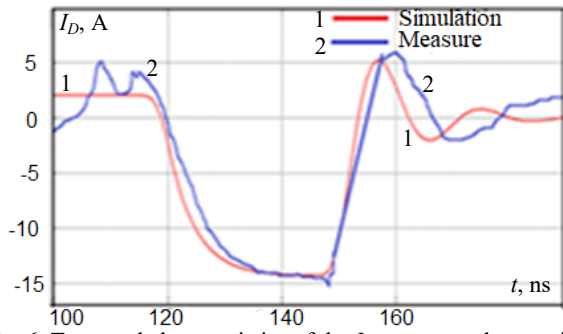


Fig. 6. Temporal characteristics of the I_D current at the opening of the diode

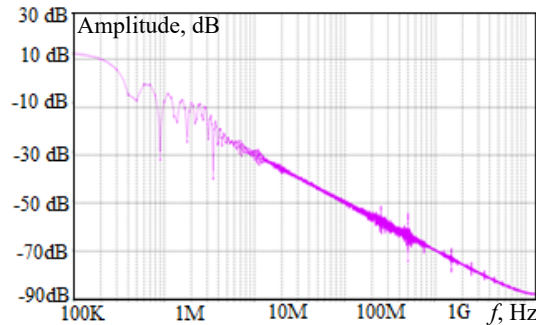


Fig. 7. Frequency characteristics of the I_D current at the opening of the diode

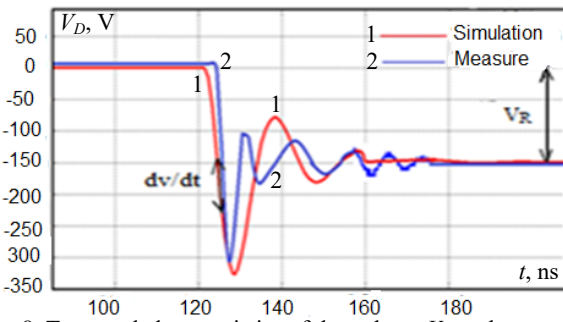


Fig. 8. Temporal characteristics of the voltage V_D at the opening of the diode

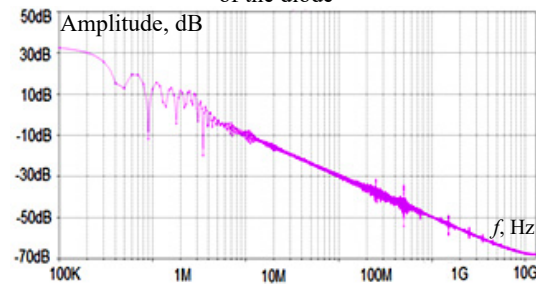


Fig. 9. Frequency characteristics of the voltage V_D at the opening of the diode

From Fig. 6, 8, we notice a good agreement between the simulation results and the experimental measurements. We can extract the transient parameters of the studied diode such as: V_{RM} – maximum reverse voltage; I_{RM} – maximum reverse recovery current of the diode; t_{RR} – reverse recovery time. At the beginning, a current I_f flows in the power diode. From the conduction of the MOSFET (M: closed switch, $V_{DS} = 0$), the current in the diode starts to decrease from the value $I_f = I_D$ with a slope:

$$\frac{di(t)}{dt} = -\frac{V_R}{L_D} \quad (3)$$

The slope is imposed by the inductance L_D (V_D is negligible compared to V_R). We obtain the following results: $I_{RM} = 14,5$ A; $t_{RR} = 38$ ns; $V_{RM} = 340$ V.

At the end of recovery, the diode then behaves as a nonlinear capacitor in series with the inductance and resistance of the circuit, resulting in a damped oscillatory response of the system with a rapid decay of the current.

We have therefore defined with these results the transient parameters describing the switching at the opening of the diode. It appears clearly the transient oscillatory phenomenon whose period is of the order of the hundred of nanoseconds.

For the frequency responses shown in Fig. 7, 9, we notice from the conduction of the MOSFET of frequency 300 kHz, an electromagnetic disturbance created between -20 dB and 20 dB due to the variation of current and voltage.

Study of the behavior of MOSFET transistor.

Figure 10 shows the electrical circuit used to record the dynamic characteristics of the MOSFET. In this simulation circuit, the inductance L_d represents the overall parasitic inductances in the circuit that causes the oscillation when the MOSFET opens [15-19]. The simulation results will be validated by experimental measurements carried out on the experimental bench shown in Fig. 4.

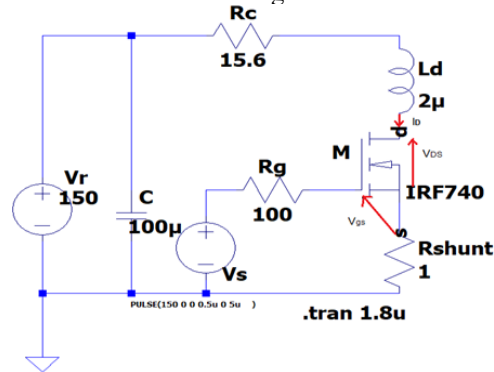


Fig. 10. Simulation scheme used to identify the dynamic parameters of the IRF740 MOSFET

According to the diagram presented in Fig. 10, we can establish the equations that describe the mesh of this circuit. The opening of the MOSFET starts with a decrease of the control voltage to zero. Consequently, the voltage across this component increases from 0 V to V_R . In this phase, the current growth rate can be expressed by (4) linking the voltage V_{DS} , V_R , and the resistances R_c and R_{shunt}

$$\frac{di(t)}{dt} = \frac{V_R - V_{RC} - V_{Rshunt} - V_{DS}}{L_D} \quad (4)$$

Results and analysis. The waveforms of the current and voltage across the MOSFETs during their opening are presented in Fig. 11, 13. The results of the simulations are validated with the realized measurements. For the frequency response, the results are shown in Fig. 12, 14. The simulated scheme has the following characteristics: $R_g = 100$ Ω , $R_c = 15,6$ Ω , $L_D = 2$ μ H, $V_R = 150$ V, $R_{shunt} = 1$ Ω .

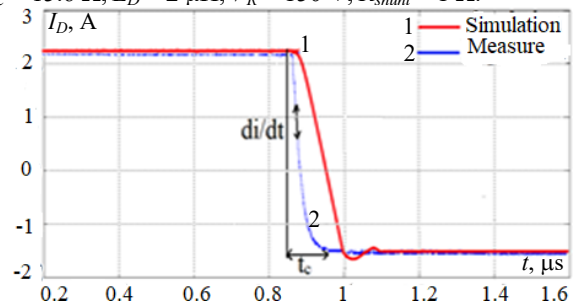


Fig. 11. Temporal characteristics of the I_D current at the opening of the MOSFET

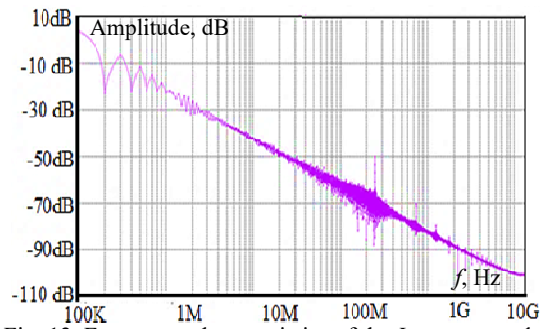


Fig. 12. Frequency characteristics of the I_D current at the opening of the MOSFET

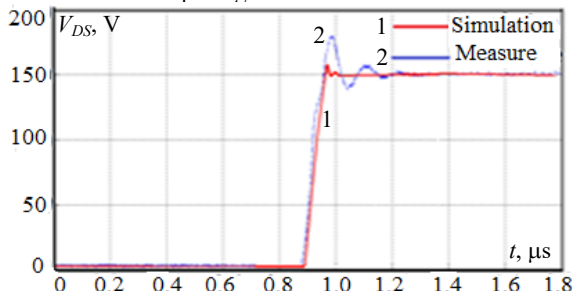


Fig. 13. Temporal characteristics of the V_{DS} voltage at the opening of the MOSFET

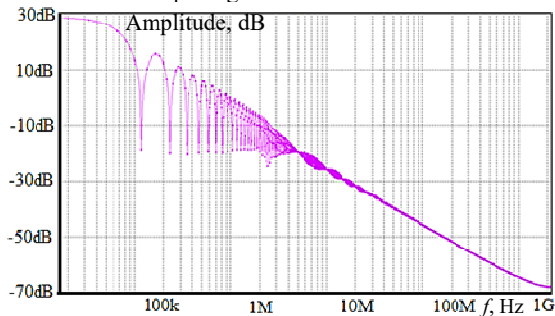


Fig. 14. Frequency characteristics of the V_{DS} voltage at the opening of the MOSFET

From the results illustrated in Fig. 11, 13, we notice that the switching of the MOSFET causes an overvoltage with an overshoot $V_{max} = 170$ V and a switching time t_c very reduced, of the order of ns which implies very important dv/dt and di/dt . In addition, an oscillatory phenomenon appears after the opening of the MOSFET. This phenomenon is explained by the effect of the connection inductance in the circuit. It can be said that the oscillatory and steep-edge phenomena of current and voltage are the cause of electromagnetic disturbances in electronic devices. For EMC problems, it is therefore essential to define the dv/dt and di/dt and the evolution of the current I_D and the voltage V_{DS} during the switching of the active components.

From the frequency results illustrated in Fig. 12, 14, we notice respectively a decrease of amplitude from 10 dB to -100 dB for the current and for the voltage a decrease of amplitude from 30 dB to -70 dB. We see in Fig. 14 that from 30 dB to -30 dB, there is a slight disturbance for the voltage V_{DS} .

Study of the behavior of the IGBT transistor. Figure 15 shows the electrical circuit used to identify the dynamic characteristics of the IGBT under Lt-spice software.

The experimental bench used for the switching of the IGBT remains the same used in Fig. 4, except that the MOSFET must be replaced by the IGBT transistor of type APT 25GF100BN, in order to visualize the voltage across the IGBT transistor and the current flowing through.

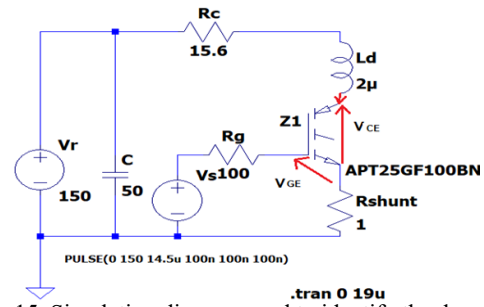


Fig. 15. Simulation diagram used to identify the dynamic parameters of the IGBT transistor

The study of dynamic behavior of the power IGBT transistor in a switching cell allowed us to define the transient and frequency parameters of the latter to represent the switching phase. The IGBT transistor used in this study is type of APT25GF100BN. Figures 16, 18 show the current and voltage time characteristics obtained from respectively simulation and measurements. Figures 17, 19 show the frequency characteristics of respectively the current and voltage at the opening of the APT25GF100BN IGBT.

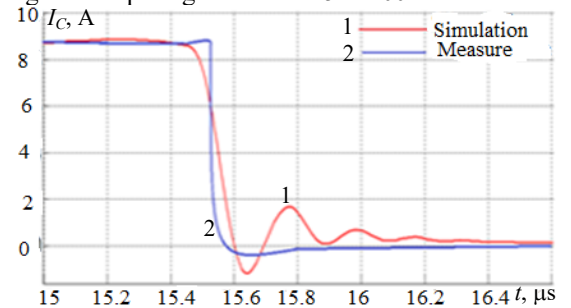


Fig. 16. Transient characteristics of the I_C current when the IGBT transistor is open

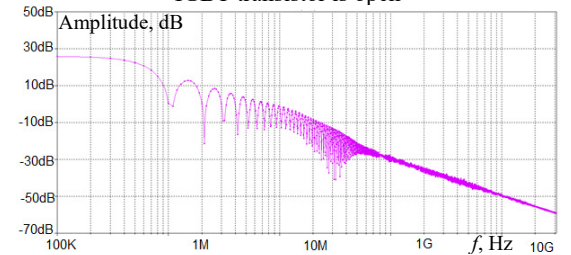


Fig. 17. Frequency characteristics of the I_C current at the opening of the IGBT transistor

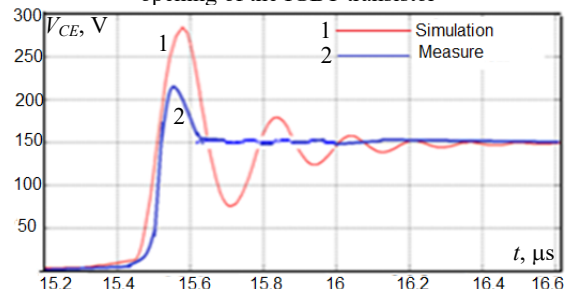


Fig. 18. Temporal characteristics of the voltage V_{CE} at the opening of the IGBT transistor

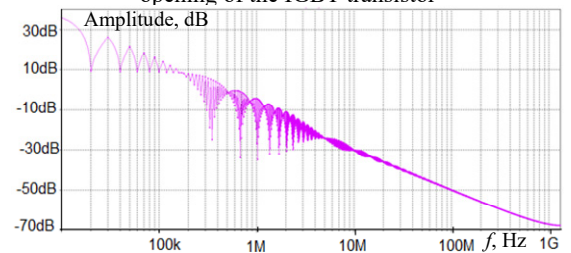


Fig. 19. Frequency characteristics of the V_{CE} voltage at the opening of the IGBT transistor

In the simulations carried out, we considered the values of the following parameters: $R_g = 100 \Omega$, $R_c = 15.6 \Omega$, $L_D = 2 \mu\text{H}$, $V_R = 150 \text{ V}$, $R_{shunt} = 1 \Omega$.

In this study, we used the same switching cell of the MOSFET, so the waveform of the current and the voltage at the terminals of the IGBT transistor remains similar to those of the MOSFET (temporal and frequency), what changes are the amplitudes and the frequency of these waves. The aspects of the dynamic behavior of an IGBT are similar to those of a MOSFET.

Conclusions.

1. Numerous electromagnetic disturbances mainly due to fast switching of the semiconductors. The disturbances propagate towards the power source of the converter and towards the load that it feeds and a part of this energy is radiated.

2. An experimental evaluation was presented in this work compared by simulation results in order to better present the influence of the fast switching of semiconductors on the electrical quantities, which causes electromagnetic disturbances in the interconnected electrical system.

3. These disturbances can be minimized by using an optimized EMC filter according to the international standards of our future work.

Acknowledgement. The authors of this article would like to thank the General Directorate of Scientific Research and Technological Development (DGRSDT) in Algeria for their technical support and the specific research budget allocated to this program.

Conflict of interest. The authors declare that they have no conflicts of interest.

REFERENCES

1. Santos V.D. *Modélisation des émissions conduites de mode commun d'une chaîne électromécanique: Optimisation paramétrique de l'ensemble convertisseur filtres sous contraintes CEM*. These de Institut National Polytechnique de Toulouse, Spécialité génie Electrique, 2019. (Fra).
2. Benhadda N., Bendaoud A., Chikhi N. A conducted EMI noise prediction in DC/DC converter using a frequency-domain approach. *Elektrotehniski Vestnik/Electrotechnical Review*, 2018, vol. 85, no. 3, pp. 103-108.
3. Chikhi N., Bendaoud A. Evaluation of Conducted Disturbances Generated by the Chopper-rectifier Association Propagating to the Electrical Network. *European Journal of Electrical Engineering*, 2019, vol. 21, no. 1, pp. 1-6. doi: <https://doi.org/10.18280/ejee.210101>.
4. Moreau M. *Modélisation haute fréquence des convertisseurs d'énergie. Application à l'étude des émissions conduites vers le réseau*. PHD Thesis, Electrical Engineering, Central School of Lille-France, 2009. (Fra).
5. Fakhfakh L., Ammous A. New simplified model for predicting conducted EMI in DC/DC converters. *Electrical Engineering*, 2017, vol. 99, no. 3, pp. 1087-1097. doi: <https://doi.org/10.1007/s00202-016-0474-2>.
6. Fakhfakh L., Alahdal A., Ammous A. Fast modeling of conducted EMI phenomena using improved classical models. *2016 Asia-Pacific International Symposium on Electromagnetic Compatibility (APEMC)*, 2016, pp. 549-552. doi: <https://doi.org/10.1109/APEMC.2016.7522795>.
7. Haque M.E., Bokhari A.A., Alolah A.I. Simulink modeling of the problem associated with fast switching PWM IGBT-inverter fed AC motor drive with long cable and its remedies. *IEEE International Conference on Systems, Signals & Devices*, 2005.
8. Boroyevich D., Zhang X., Bishnoi H., Burgos R., Mattavelli P., Wang F. Conducted EMI and systems integration. *CIPS 2014 8th International Conference*, Nuremberg, 2014.

How to cite this article:

Slimani H., Zeghoudi A., Bendaoud A., Bechekir S. Experimental evaluation of conducted disturbances induced during high frequency switching of active components. *Electrical Engineering & Electromechanics*, 2023, no. 5, pp. 26-30. doi: <https://doi.org/10.20998/2074-272X.2023.5.04>

9. Ales A., Gouichiche Z., Schanen J.-L., Roudet J., Boudaren M.E.Y., Karouche B., Moussaoui D. The accurate input impedances of a DC-DC converters connected to the network. *2015 IEEE 15th International Conference on Environment and Electrical Engineering (EEEIC)*, 2015, pp. 331-336. doi: <https://doi.org/10.1109/EEEIC.2015.7165183>.
10. Slimani H., Zeghoudi A., Bendaoud A., Reguig A., Benazza B., Benhadda N. Experimental Measurement of Conducted Emissions Generated by Static Converters in Common and Differential Modes. *European Journal of Electrical Engineering*, 2021, vol. 23, no. 3, pp. 273-279. doi: <https://doi.org/10.18280/ejee.230312>.
11. Zeghoudi A., Bendaoud A., Slimani H., Benazza B., Bennouna D. Determination of electromagnetic disturbances in a buck chopper. *Australian Journal of Electrical and Electronics Engineering*, 2022, vol. 19, no. 2, pp. 149-157. doi: <https://doi.org/10.1080/1448837X.2021.2023073>.
12. Mahesh G., Subbarao B., Karunakaran S. Effect of power frequency harmonics in conducted emission measurement. *Proceedings of the International Conference on Electromagnetic Interference and Compatibility*, 2008, pp. 273-277.
13. Seguier G., Labrique F., Delarue P. *Electronique de puissance. Structures, commandes, applications*, 10e edition, Dunod, Paris, 2015. 425 p. (Fra).
14. Duan Z., Fan T., Zhang D., Wen X. Differential Mode Conducted EMI Prediction in Three Phase SiC Inverters. *IOP Conference Series: Materials Science and Engineering*, 2017, vol. 199, art. no. 012126. doi: <https://doi.org/10.1088/1757-899X/199/1/012126>.
15. Mrad R., Morel F., Pillonnet G., Vollaire C., Lombard P., Nagari A. N-Conductor Passive Circuit Modeling for Power Converter Current Prediction and EMI Aspect. *IEEE Transactions on Electromagnetic Compatibility*, 2013, vol. 55, no. 6, pp. 1169-1177. doi: <https://doi.org/10.1109/TEMC.2013.2265048>.
16. Fedyczak Z., Kempinski A., Smoleński R. Conducted high frequency disturbances observed in electrical power systems with switch mode converters. *Przeglad Elektrotechniczny*, 2013, vol. 89, no. 6, pp. 41-50.
17. Zeghoudi A., Slimani H., Bendaoud A., Benazza B., Bechekir S., Miloudi H. Measurement and analysis of common and differential modes conducted emissions generated by an AC/DC converter. *Electrical Engineering & Electromechanics*, 2022, vol. 4, pp. 63-67. doi: <https://doi.org/10.20998/2074-272X.2022.4.09>.
18. Lounis Zohra. *Apports des techniques de cablages laminaires dans un onduleur a IGBT de moyenne puissance*. These de doctorat, Institut National Polytechnique de Lorraine, 2000. (Fra).
19. Marlier C. *Modélisation des perturbations électromagnétiques dans les convertisseurs statiques pour des applications aéronautiques*. These de doctorat, en Génie électrique Université Lille Nord-de-France, 2013. (Fra).

Received 09.08.2022

Accepted 12.12.2022

Published 01.09.2023

Helima Slimani,^{1,2} Lecturer,
Abdelhakim Zeghoudi¹, PhD,
Abdelber Bendaoud¹, Professor,
Seyf Eddine Bechekir¹, Lecturer,
¹Laboratory of Applications of Plasma, Electrostatics and
Electromagnetic Compatibility (APELEC),
Djillali Liabes University of Sidi Bel-Abbes, Algeria,
e-mail: hakooumzeghoudi@gmail.com;
b Abdelber@gmail.com (Corresponding Author);
seyfeddine.electrotechnique@gmail.com
²University of Tiaret, Algeria,
e-mail: halima.slimani@univ-tiaret.dz